

# Computational Fluid Dynamics Simulation of Drag Reduction by Riblets on Automobile

N.N.N. Ghazali, Y. H. Yau\*, A. Badarudin and Y.C. Lim

*Department of Mechanical Engineering,  
University of Malaya, 50603 Kuala Lumpur, Malaysia.  
Corresponding email: [yhyau@um.edu.my](mailto:yhyau@um.edu.my)*

**Abstract.** One of the ongoing automotive technological developments is the reduction of aerodynamic drag because this has direct impact on fuel reduction, which is a major topic due to the influence on many other requirements. Passive drag reduction techniques stand as the most portable and feasible way to be implemented in real applications. One of the passive techniques is the longitudinal microgrooves aligned in the flow direction, known as riblets. In this study, the simulation of turbulent flows over an automobile in a virtual wind tunnel has been conducted by computational fluid dynamics (CFD). Three important aspects of this study are: the drag reduction effect of riblets on smooth surface automobile, the position and geometry of the riblets on drag reduction. The simulation involves three stages: geometry modeling, meshing, solving and analysis. The simulation results show that the attachment of riblets on the rear roof surface reduces drag coefficient by 2.74%. By adjusting the attachment position of the riblets film, reduction rates between the range 0.5%-9.51% are obtained, in which the position of the top middle roof optimizes the effect. Four riblet geometries are investigated, among them the semi-hexagon trapezoidally shaped riblets is considered the most effective. Reduction rate of drag is found ranging from -3.34% to 6.36%.

**Keywords:** Riblets, Drag Reduction, CFD, Semi-Hexagon Trapezoidally Shaped Riblets  
**PACS:** 47.11.-j

## INTRODUCTION

Drag coefficient is very important to take into account when conceiving an automobile since it influences engine requirements, fuel consumption and the overall aerodynamic performance. It has been shown that forty percent of the drag coefficient depends on the external shape and most of it is at the rear of the geometry. Wake structure at the rear-end shape of the vehicle is the major cause of aerodynamic drag [1]. By controlling the laminar-turbulent transition, wall shear stress, wake and flow separation, the drag coefficient can be minimized. Riblets are micro-grooves on the surface which aligned to the free stream direction. For typical triangular riblets, skin friction drag is reduced by up to 8% [2]. Although riblets are quite tolerant to misalignment of the flow, drag reduction is completely lost when the yaw angle exceeds about 30°. The net skin friction is almost linearly proportional to the amount of coverage of riblets over the body surface, suggesting that the turbulent drag reduction is a predominantly local phenomenon. Recent research has made considerable improvement in drag reduction by optimizing the geometry of riblets. As a result, drag reductions of as much as 10% or more can now be achieved using highly optimised geometry [3]. The objectives of this study are to compare the aerodynamic drag with and without the riblets, to investigate the effectiveness of riblets on different positions on the vehicle's body surface and to study the effectiveness of riblets of different geometries.

Nomenclature:			
CFD	Computer Fluid Dynamics	$\rho$	Density
$V$	Velocity	$A$	Projected Area
$I$	Turbulence intensity	$C_{SM}$	Drag coefficients of smooth surface model
$D_h$	Hydraulic diameter	$C_{RM}$	Drag coefficients of riblets model
$\frac{\partial \psi}{\partial n}$	Gradient of physical parameter	$\Delta h$	Height difference
$C_v$	Force coefficient	$s^+$	Rib lateral spacing,
$C_p$	Pressure force	$h/s$	Ratio of rib height to rib spacing,

## METHODOLOGY

Except for the original automobile model, the other five models were mounted with riblets on its body surfaces. The positions identified for investigation are the front of car, the front of roof, the rear of roof, the rear end of car and the side door. For convenience, the five positions hereafter will be referred as Position A, Position B, Position C, Position D and Position E. Each riblet film covers an area of  $0.5\text{m} \times 0.05\text{m}$  as shown in Figure 1. The dimensions of four geometries that are used for investigation about the effect riblets geometry on drag reduction are shown in Figure 2. They are referred to as Geometry A (wedge), Geometry B (square), Geometry C (semi-sphere) and Geometry D (semi-hexagon). All the riblets of different geometry are fixed on Position A. Totally; there are 9 case models to be studied for this project.

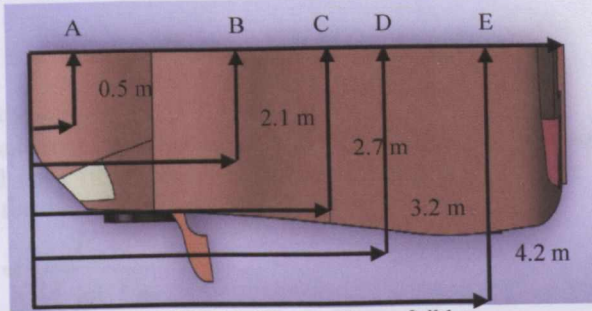


FIGURE 1. The positions of riblets

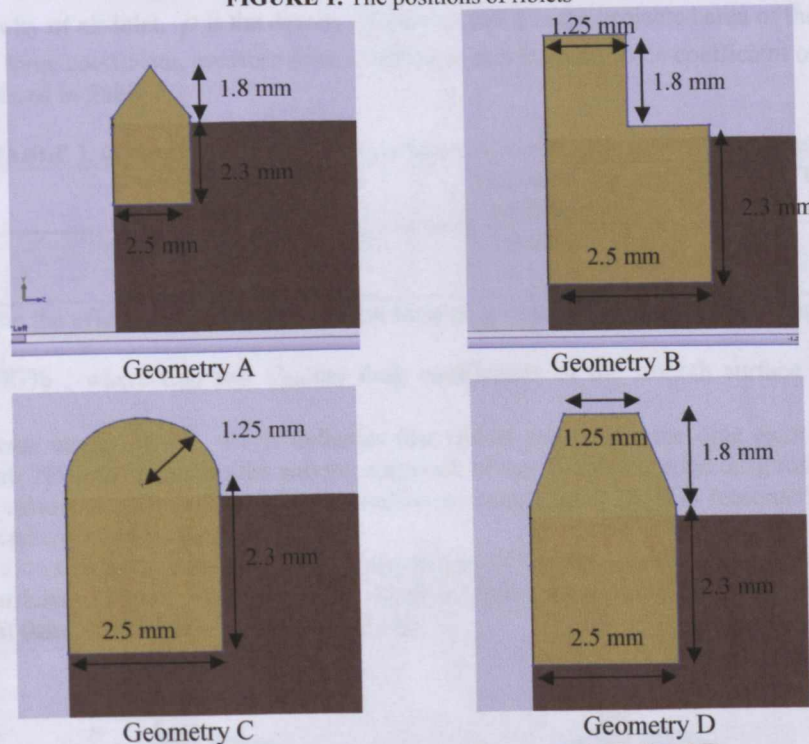


FIGURE 2. Geometry of riblets used: Geometry A, B, C and D.

### Velocity inlet

Velocity inlet boundary conditions were used to define the flow velocity, along with all relevant scalar properties of the flow, at flow inlets. This boundary condition is intended for incompressible flows, and its use was appropriate for this case. The inlet velocity was set as  $V = 35\text{ms}^{-1}$ , the approximate to that used in previous experimental works. This value of velocity is also in the range of low speeds (35-45 m/s) which significantly shows the drag reduction by riblets.

Turbulence Specification Method of velocity inlet setting specifies the method to input the turbulence parameters. Turbulence Intensity and Hydraulic Diameter method are chosen because it was assumed that the model was in a virtual wind tunnel where the flow is internally fully developed. For internal flows, the turbulence intensity at the inlets is totally dependent on the upstream history of the flow. If the flow upstream is under-developed and undisturbed, low turbulence intensity can be used. Turbulence intensity is given as  $I = 0.16(\text{Re}_{dh})^{-1/8}$ . This work simulated the test of the low speed wind tunnel, so the turbulence intensity  $I$  is dependent on the parameter of the low speed wind tunnel,  $I = 0.4\%$  [4]. The hydraulic diameter  $D_h$  is selected as another turbulence parameter,  $D_h = 7.87\text{m}$ .

## Outflow

Outflow boundary condition in FLUENT was used to model flow exits where the details of the flow velocity and pressure are not known prior to solution of the flow problem. Outflow was used because this study dealt with an incompressible, steady flow with constant density and the inlet was not a pressure inlet. The outlet condition is that the turbulence is developed sufficiently and the gradient of physical parameter is zero, i.e.  $\frac{\partial \psi}{\partial n} = 0$ . The outflow boundary was situated far enough downstream from the vehicle so that the outflow conditions have no impact on the flow field in the vicinity of the vehicle.

## RESULTS AND DISCUSSION

### Effect of Riblets on Drag Reduction

Applying CFD simulations, the viscous force coefficient  $C_v$ , and the pressure force,  $C_p$ , exerted on the smooth surface models and on a riblet model (Position D, Geometry A) were obtained. The viscous force coefficient and the pressure force coefficient are defined as:

$$C_v = \frac{F_v}{\frac{1}{2} \rho V^2 A} \text{ and } C_p = \frac{F_p}{\frac{1}{2} \rho V^2 A} \quad (1)$$

where  $V$  is the velocity of air inlet,  $\rho$  is the density of the air, and  $A$  is the projected area of the model on the  $y$ - $z$  plane. The viscous force coefficient, pressure force coefficient and the total force coefficient of both smooth and riblets models are listed in Table 1.

TABLE 1. Comparison of drag coefficient between smooth surface and riblets model

Model	Pressure force coefficient	Viscous force coefficient	Total force coefficient
Smooth surface	0.3355	0.0262	0.3617
Riblets	0.3314	0.0203	0.3518

To examine the effect of the riblets model on total drag reduction, the drag reduction rate is defined as  $\frac{C_{SM} - C_{RM}}{C_{SM}} \times 100\%$ , where  $C_{SM}$  and  $C_{RM}$  are drag coefficients of the smooth surface model and riblets

model. The reduction rate is 2.74%, which indicates that riblets can reduce the drag exerting on automobile under low air speed. This result verifies the solving approach of this study, since the drag reduction by riblets is proven in various researches. The values of drag coefficient simulated, 0.36, also reasonably close to the real Lamborghini Murcielago LP640's 0.33.

Table 1 shows that for both models, the major part of the drag coefficient is attributed to pressure viscous force coefficient (Figure 3). It was also observed that riblets are more efficient on viscous drag reduction (22.52%) than pressure drag reduction (1.22%).

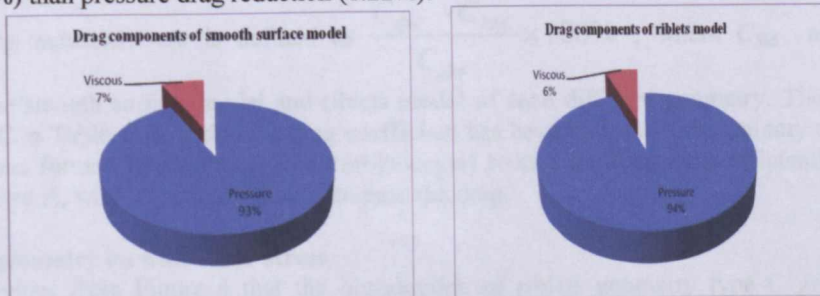


FIGURE 3. Drag components for smooth surface and riblets model.

The values of pressure and viscous drag force for both models are shown in Table 2. The drag force reduction rate was calculated as its drag coefficient counterpart, and found to be 2.6%. Both rates are quite close, and according to Equation 1, the drag coefficient and drag force are proportional to each other. Hence, the subsequent discussion will focus on the drag coefficient parameter only.

TABLE 2. Comparison of drag force between smooth surface and riblets model

Model	Pressure force (N)	Viscous force (N)	Total force (N)
Smooth surface	418.03	32.66	450.68
Riblets	411.00	27.96	438.96

### Effect of Riblets Position on Drag Reduction

The previous results have proven that riblets could reduce the drag of a vehicle, and the solving model of this study has been verified. The second part of the discussion will focus on how the different locations of riblets to be placed have influenced the drag reduction. Five positions has been identified and used for this investigation. The results of simulation of each model are tabulated below:

**TABLE 3.** Comparison of drag coefficient and reduction rate of different positioned riblets.

MODEL	PRESSURE FORCE COEFFICIENT	VISCOUS FORCE COEFFICIENT	TOTAL FORCE COEFFICIENT	REDUCTION RATE (%)
Smooth	0.3355	0.0262	0.3617	-
Position A	0.3398	0.0201	0.3599	0.50
Position B	0.3149	0.0207	0.3356	7.22
Position C	0.3054	0.0219	0.3273	9.51
Position D	0.3314	0.0203	0.3518	2.74
Position E	0.3224	0.0210	0.3434	5.06

The drag reduction rate is defined as  $\frac{C_{SM} - C_{RM}}{C_{SM}} \times 100\%$ , where  $C_{SM}$  and  $C_{RM}$  are drag coefficients

of the smooth surface model and riblets model of each different position. The positions, from A to E, are shown in Figure 1 above. Relating the location of these positions with the calculated reduction rate, it is observed that the reduction rate is the lowest near the front of the car, increasing until the mid of the car (position E), and finally fluctuating from A to D. It is interesting to note that apparently there is no proportionality occurs between these positions and the reduction rate, thus a further analysis is required to find out their relationship.

### Effect of Riblets Geometry on Drag Reduction

For this section, various riblet geometries are simulated to investigate its performance on drag reduction. Four geometries are chosen, referred as Geometry A (wedge), Geometry B (square), Geometry C (semi-sphere) and Geometry D (semi-hexagon).

**TABLE 4.** Reduction rates of different riblet geometries

Model	Pressure Force Coefficient	Viscous Force Coefficient	Total Force Coefficient	Reduction Rate (%)
Smooth	0.3355	0.0262	0.3617	-
Geometry A	0.3314	0.0203	0.3518	2.74
Geometry B	0.3481	0.0205	0.3686	-1.91
Geometry C	0.3533	0.0205	0.3738	-3.34
Geometry D	0.3179	0.0207	0.3387	6.36

The drag reduction rate is defined as  $\frac{C_{SM} - C_{RM}}{C_{SM}} \times 100\%$ , where  $C_{SM}$  and  $C_{RM}$  are drag

coefficients of the smooth surface model and riblets model of each different geometry. The reduction rates of geometry B and C in Table 4 show that the drag coefficient has been increased. Preliminary result indicates that the sharp V-groove formed by Geometry D (semi-hexagon) reduce the drag most efficiently, followed by V-groove of Geometry A, while B and C slightly increase the drag.

### Effect of riblet geometry on wall shear stress

It is obvious from Figure 4 that the introduction of riblets geometry type C greatly increases the turbulent wall shear stress, to a level approaching 8.5 Pa. While the other 3 types of riblets are steady in maintaining shear stress in range 0.5-5 Pa, with the most efficient by geometry D, followed by B then A.

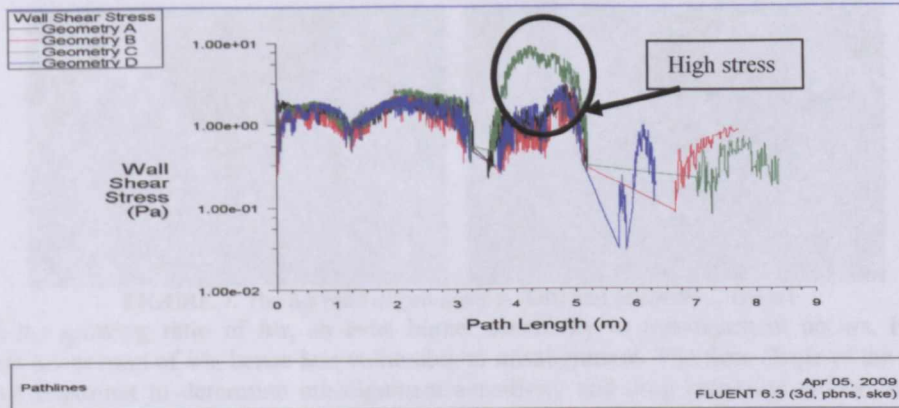


FIGURE 4. Pathlines plot of wall shear stress for different geometry models.

Hampering the velocity in lateral direction will reduce momentum transfer and skin friction, such that align the riblets in the mean flow direction. Second, the protrusions should not higher than  $y^+ \approx 5$ , which will increase the drag. Third, the protrusion height difference,  $\Delta h$  is required to be maximized for higher drag reduction.

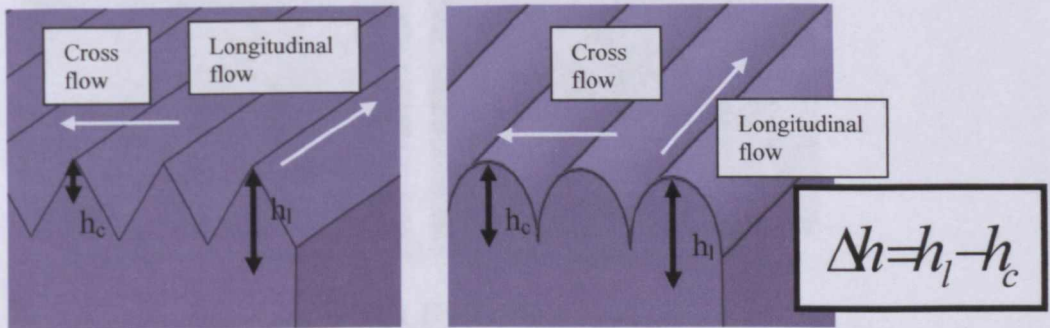


FIGURE 5. Protrusions height difference of riblets Geometry A and C

From the 3 factors above, all the 4 geometries of riblets do reduce airflow speed and have the riblets height from 1.25 mm to 1.8 mm, with  $y^+$  of C lower than A in this comparison. The only factor differentiate them is the protrusion height. When experiencing cross flow, the virtual origin of geometry C cannot remains near to tips due to its sphere shape, results in higher  $h_c$ , hence its drag reduction function deteriorates.

#### Riblet geometry and misalignment vulnerability

It is important to understand the deteriorating effect of misalignment because deviations in flow direction do occur at varying angle of attack of the surface. Three geometric quantities are responsible for the sensitivity to misalignment: the rib lateral spacing,  $s^+$ , the ratio of rib height to rib spacing,  $h/s$ , and the shape of the cross section valley between two ribs.

The spacing of riblets in different geometries used in this study is the same, that is 2.5 mm. For a given ratio of  $h/s = 0.5$ , the trapezoidally grooved riblets with smaller groove angle will perform better. Comparing the two trapezoidally and triangularly grooved of the study models here, the groove angle of geometry D is smaller, hence it is believed that it has the advantage in this prospect.

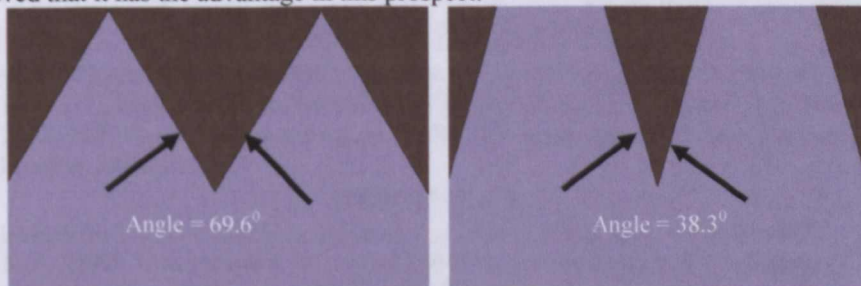


FIGURE 6. Groove angle of geometry A (left) and geometry D (right)

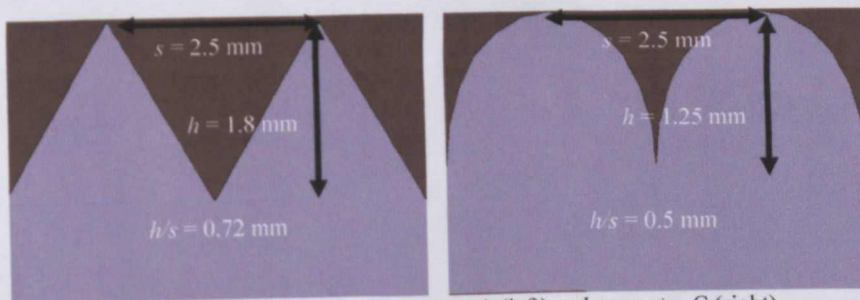


FIGURE 7. The  $h/s$  ratio of geometry A (left) and geometry C (right)

With the growing ratio of  $h/s$ , an even higher sensitivity to misalignment occurs. From Figure 7, geometry C has lower ratio of  $h/s$ , hence less vulnerable to misalignment. The floor shape of the valley between the ribs is also important to determine misalignment sensitivity and drag reduction ability. A narrow notch performs slightly better in terms of insensitivity to misalignment than broad floor. One likely reason for this is the phenomenon that the fluid in the valleys tends to slosh. Sloshing is a lateral movement of fluid in between the ribs, which produces a motion normal to the wall. This additional momentum exchange is responsible for additional losses in drag reduction, and its appearance is more likely for broader valleys, such as the one formed by geometry B.

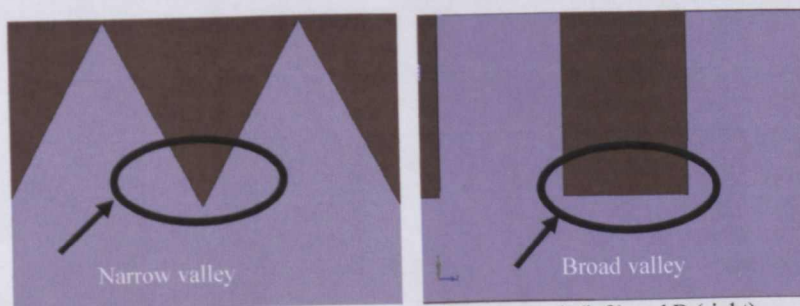


FIGURE 8. Floor shape of the valley of geometry A (left) and B (right).

## CONCLUSIONS

Throughout the study, two main sources of drag were encountered and identified. The first drag term is called the form drag, which is also referred to as pressure drag, caused by the adverse pressure gradient of the flow domain around the automobile. The second source of drag is the friction drag, caused by the wall shear stress of the air flow through the surface of the automobile. Using the wedge shape riblets with a triangular cross-section attached on the rear roof of the automobile, the effect of the riblets has been studied. The drag coefficient of a smooth surface model is simulated to be 0.3617, while the use of wedge riblets was found to have drag reduction rate of 2.74%. The position of riblets attached on top of the middle roof of the automobile was found to be the most ideal, as far as drag reduction is concerned. A reduction rate as high as 9.51% was recorded for this position, while several more positions were investigated and the corresponding reduction rate falls in the range of 0.5-7.22%. The riblets on middle roof (referred as position C) is discovered to have better performance on reducing pressure gradient, vorticity and turbulence intensity, inducing lower wall shear stress, restricts the airflow speed and less susceptible to yaw angle effect. Among the four geometries of riblets investigated, the semi-hexagon trapezoidally shaped riblets, with narrow V-grooves (geometry D), was found to be the best. A drag reduction rate of 6.36% was obtained from this geometry, while the semi-circular and square cross section geometries reported to have increased the drag.

## ACKNOWLEDGMENTS

The authors would like to acknowledge the full financial assistance from the Ministry of Science, Technology and Innovation (MOSTI), Malaysia, via e-Science Fund Project 13-02-03-3034 and University of Malaya (UM) PJP Grants FS126/2008B, FS131/2008B and FS219/2008A for research work to be conducted in University of Malaya, Kuala Lumpur, Malaysia.

## REFERENCES

1. Wolf-Heinrich Hucho. (1997). *Aerodynamics of road vehicles*. 4<sup>th</sup> Ed. London: Butterworth.
2. Walsh M.J. (1980). Drag reduction of V-groove and transverse curvature riblets. *Viscous flow drag reduction, Progress in Astronautics and Aeronautics*. 72. 168-184.
3. Thiede Peter. (2001). Industrial Perspectives of Drag Reduction Technologies. *Aerodynamic Drag Reduction Technologies: Proceedings of the CEAS/DragNet European Drag Reduction Conference, 19-21 June 2000, Potsdam, Germany*. 76. 259-266. /
4. Tian L.R., Red L.Q., Lid Q.P., Had Z.W., Xiao Jiang. (2007). The Mechanism of Drag Reduction around Bodies of Revolution Using Bionic Non-Smooth Surfaces. *Journal of Bionic Engineering*. 4. 109-116.